RESEARCH PAPER

Investigation on Microstructure Evolution of a Semi-Austenitic Stainless Steel Through Hot Deformation

S. Mortezaei[1], H. Arabi[1*], S. H. Seyedein[1] , A. Momeni[2] and M. Soltanalinezhad[3]

** arabi@iust.ac.ir*

Received: December 2019 Revised: April 2020 Accepted: May 2020

[1] Department of Metallurgical Engineering, Iran university of science & technology, Tehran, Iran.
[2] Department of Metallurgical Engineering, Hamedan university of technology, Hamedan, Iran.
[3] Department of Metallurgical Engineering, Amirkabir university of technology, Tehran, Iran.

DOI: 10.22068/ijmse.17.3.60

Abstract: *Dynamic Recrystallization (DRX) is one of the likely mechanisms for fine-graining in metals and alloys. The dynamic recrystallization (DRX) phenomena occur in different thermo-mechanical processing (TMP) conditions for various metallic materials. DRX depends on various materials and thermo-mechanical parameters such as temperature, strain rate, strain, stress, and initial microstructure. in the present study, the restoration mechanism of the 17-7PH stainless steel has been investigated using a hot compression test under different conditions of thermo-mechanical treatment. The microstructural characteristics and the behavior of the hot deformation of the understudy steel are investigated using flow curves and microstructure images obtained from optical microscopy. The results show that the maximum and steady-state stresses are significantly affected by the strain rate and the deformation temperature. So, the flow stress increases with a decrease in the deformation temperature and an increase in the strain rate. Microstructural studies confirm the occurrence of DRX as a restoration mechanism in the microstructure for the two phases of austenite and ferrite.*

Keywords: *Dynamic Recrystallization, Thermo-mechanical processing, 17-7PH Stainless steel, Compression test.*

1. INTRODUCTION

Restoration mechanisms in metals during hot work have been one of the main issues in recent decades. In most cases, dynamic recovery has been reported as the only restoration mechanism for alloys with high stacking fault energy (SFE) [1-2]. Besides, in metals and alloys with high SFE, continuous dynamic recrystallization (CDRX) occurs instead of discontinuous dynamic recrystallization (DDRX). CDRX plays a prominent role in producing finer grains through hot deformation [3-5]. This mechanism mostly occurs in low carbon ferritic steels [6-7], and even to some extent in austenitic stainless steels [8-10]. Generally speaking, ferritic microstructures prefer the work softening by an extended dynamic recovery which results in CDRX at higher applied strains. Dynamic restoration leads to an increase in the density of dislocations at low-angle grain boundaries (LAGBs) thereby transforming them into high-angle grain boundaries (HAGBs). It is generally accepted that sub-grains may rotate to the point that the adjacent sub-grains reach a similar orientation due to boundary diffusion processes. In this case, already existing LAGBs will be deleted [11]. These sub-grains will combine and convert to larger subgrains. The driving force necessary for this process will be obtained by the decrease in the surface area of LAGBs in unit volume.

Ferrite and austenite behave differently during deformation at high temperatures. The diffusion rate in ferrite is greater than the austenite. Therefore, the movement of the dislocations is significantly faster in ferrite than in austenite. Austenite Instead prefers dynamic recrystallization by DDRX mechanism. DDRX happens by the nucleation and growth of new grains (mostly by the strain-induced boundary migration, SIBM) [11]. However, austenite possibly experiences CDRX under special conditions such as a lack of favorable nucleation sites and a decrease in driving force for the SIBM mechanism. For example, the decrease in high-angle austenite/austenite bound-

[DOI: 10.22068/ijmse.17.3.60]

ary in dual-phase steels may decrease the possibility of DDRX in comparison to fully austenitic structures. Therefore under these circumstances, the alternative softening mechanism, i.e. CDRX, comes into operation [12]. the occurrence of CDRX during hot deformation of super austenitic stainless steels confirms this idea [13].

17-7PH (AISI 631) stainless steel is a precipitation-hardenable stainless steel with semi-austenitic microstructure. It is the first semi-austenitic PH stainless steel that has been commercially produced. This steel contains austenite and delta ferrite (in the range of 5 to 20 %) at room temperature. Austenite in this steel is thermodynamically metastable and may transform into another phase during heat treatment or cold working. On the other hand, the amount of delta ferrite depends on ferrite promoting elements such as chromium, aluminum, and titanium. This steel has a good combination of properties such as good ductility, high strength, and great resistance to corrosion which has led its application in various applications such as nuclear powerhouses [14-15]. The addition of light elements such as aluminum has been considered as a good and interesting way for increasing strength and meanwhile decreasing the weight [16]. However, such changes in chemical composition often results in sophisticated microstructural evolution during hot working. The mechanism of microstructural evolution depends on different thermomechanical and material factors such as temperature, strain rate, strain, material nature, chemical composition, and initial microstructure. In this study, the effect of thermomechanical parameters such as strain, temperature, and strain rate on the microstructure of 17-7PH stainless steel has been investigated using hot compression tests.

2. EXPERIMENTAL PROCEDURE

The chemical composition of the steel used in this research is given in Table 1. To study the hot working behavior of the steel, cylindrical specimens of 12 mm in height and 8 mm in diameter were used.

The specimens were initially homogenized by holding at 1050 for 30 minutes and then cooled in the air. After preheating at test temperature for 5 minutes, hot compression tests were applied using a Santam tensile/compression machine equipped with a furnace at temperatures of 950 and 1050 with strain rates of 0.01 and 0.1 s^{-1} until reaching true strains of 0.15, 0.3, 0.45 and 0.6. After the hot compression tests, the deformed specimens were promptly quenched in water. The deformed specimens were then cut in the middle and etched in an electrolyte solution containing nitric acid, for 6 seconds using a voltage of 1.5 V. The etching procedure was designed to reveal the prior austenite grain boundaries rather than the martensitic structure.

3. RESULTS AND DISCUSSION

3.1. Stress-Strain Curves

The flow curves of 17-7PH stainless steel under hot working conditions are shown in Fig. 1. It is evident that the flow stress decreases with an increase in deformation temperature (Fig. 1 (a)) and a decrease in strain rate (Fig. 1 (b)). Indeed, faster diffusion at higher temperatures leads the dislocations to move more easily and the drop in flow stress is its result. This phenomenon indicates the acceleration of work softening processes with increasing deformation temperature. Also, it is observed that by increasing the deformation temperature, the stress increases to the maximum stress at a smaller strain. In fact, the maximum strain is transmitted to lower strains as temperatures rises or strain rate declines. The reduction of the maximum strain to lower strain indicates that the increase in temperature can be a factor in intensifying the occurrence of DRX [17].

By increasing the strain rate, due to reduced deformation time, the strain is applied in less time. Therefore, there is less chance for the occurrence

Table 1. Chemical composition of 17-7PH steel used in this research (wt. %)

elements	C	Cr	Ni	Mn	Si	Al	Fe
sample	0.04	17.06	7.2	0.674	0.385	1.06	Bla

[DOI: 10.22068/ijmse.17.3.60]

of dynamic recovery in the material. However, at high strain rates, there is not enough time for dislocations to join together to form sub-boundaries [18]. Therefore, at high strain rates, recovery processes are postponed and work hardening overcomes. The flow curves in Fig. 1 (a) show that the peak stress at 950 occurs at a strain almost equal to 0.4. At larger strains, i.e. 0.4- 0.6, the stress drops, and the plateau of steady-state deformation is hardly visible even at a strain of 0.6. However, at 1050, the peak stress appeared at a strain of 0.3; then the flow stress dropped and eventually reached the stable state at a strain of 0.5. This indicates that at both deformation temperatures there is a relative balance between work hardening and dynamic softening at large strains. Fig. 1 (b) indicates that the peak strain and the steady-state condition are less sensitive to strain rate than temperature. This is because the peak stress for 0.01 and 0.1 s^{-1} appears at strains of 0.4 and 0.43, respectively. Besides, the strains corresponding to the steady-state plateau are very close together.

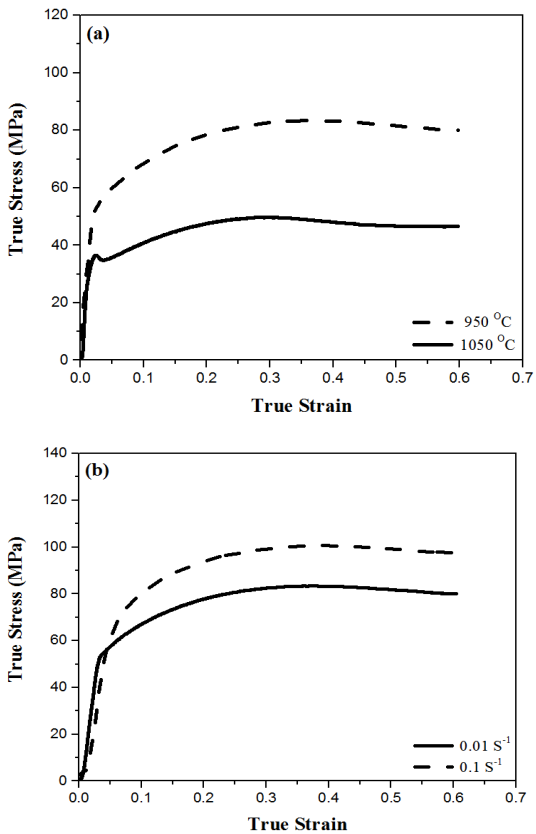

Fig. 1. True stress-strain curves of deformed specimens: a) at constant strain rate of 0.01 s^{-1} and b) at constant temperature of 950 °C.

3.2. Microstructural Studies

The initial microstructure of the 17-7PH stainless steel is shown in Fig. 2. In this microstructure, the matrix phase is austenite with the average grain size of about 42.5 µm and the co-axial ferrite phase which is visible as islands at the grain boundaries and triple junctions of austenite is delta ferrite.

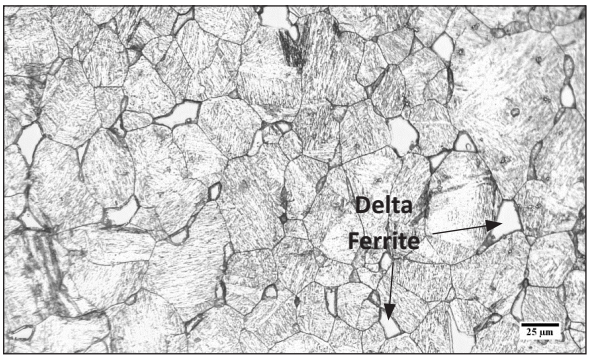

Fig. 2. Initial microstructure of 17-7PH stainless steel. The outline shows the equiaxed austenite grains revealed by the special etching method. The island phase is delta (δ) ferrite.

Fig. 3 shows the microstructure of deformed samples at 950 °C and strain rate of 0.01 s^{-1} at strains of 0.15, 0.3, 0.45, and 0.6. Fig. 3 (a) shows that the γ grains and δ islands have almost remained equiaxed at low strains. Although a strain of 0.15 is in the middle of the work hardening region of the flow curve (Fig. 1 (b)), the serrated grain boundaries (shown by the black arrows) indicate the progress of DRV in the substructure. We know that HAGBs are serrated due to the tensions of LAGBs which intersect them [11]. The appearance of serrated grain boundaries at low strains is therefore a sign of fast DRV in the studied material.

A comparison between Fig. 3 (a) and starting microstructure in Fig. 2 reveals that some small grains, presumably due to DRX, are appeared around the original grain boundaries. Failure to observe the necklace structure in the early stages of recrystallization shows that the probability of DDRX, which occurs through the nucleation and growth of new grains almost at prior grain boundaries is very weak in this alloy. Moreover, as a strain of 0.15 is well below the peak strain, around 0.3, the appearance of small grains cannot

[DOI: 10.22068/ijmse.17.3.60]

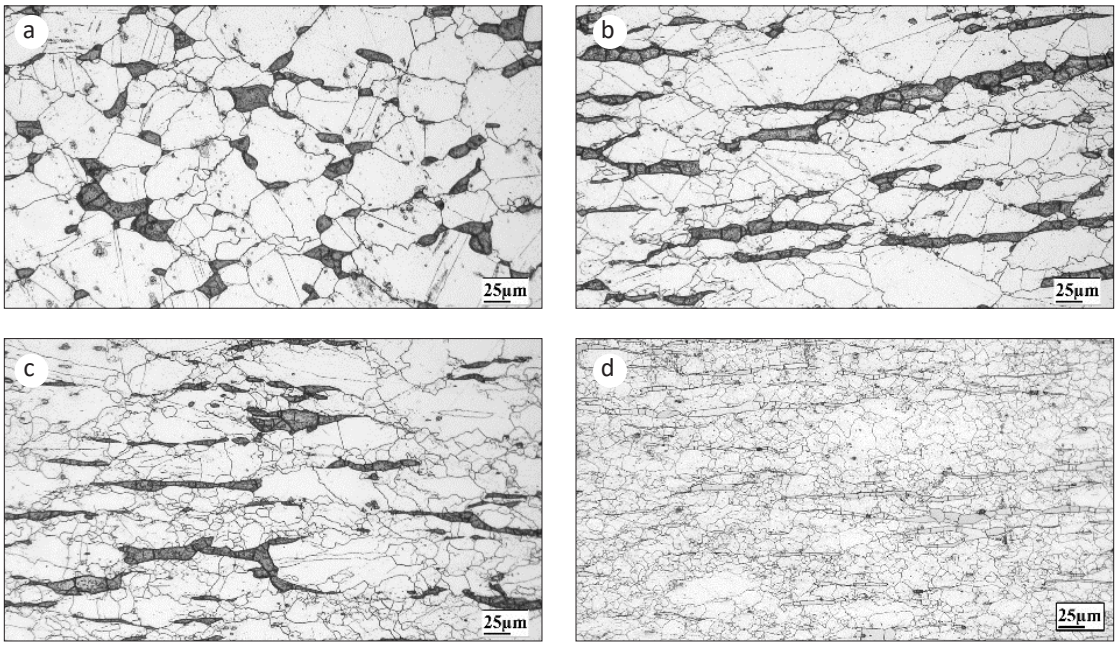

Fig. 3. Microstructure of deformed samples at 950 °C and strain rate of 0.01 s^{-1} to strain of a) 0.15, b) 0.3, c) 0.45 and d) 0.6.

be ascribed to the activation of DDRX. Alternatively, the evolution of microstructure and the appearance of serrated grain boundaries should be due to cooperation between DRV and CDRX. It should be emphasized that the major discrepancy between DDRX and CDRX is that the former needs the build-up of deformation energy (dislocation density) to be activated almost nearby the peak strain [19], while the latter can be activated by fast DRV at much lower strains. As the deformation continues to reach the peak strain (around 0.3) (Fig. 3 (b)), the original grains and δ islands are elongated and oriented perpendicular to the compression axis. The number of new CDRX grain has obviously increased. The new grains are observed everywhere, inside the original elongated grains and along the grain boundaries. Various mechanisms have been proposed for CDRX [5, 20]. Bricknell and Edington [21] suggested that the decomposition and combination of the sub-grain boundaries could lead to the formation of high-angle boundaries. Nes [22] suggested that high-angle boundaries could be as a result of the rapid growth of the sub-grains during severe plastic deformation. However, the mechanism which seems to be prevailing is the gradual rotation of sub-grains with an increase in the applied strain. Through this process, the misorientation along the sub-boundaries increases with strain until exceeds 15 °, where the transformation of well-developed sub-grain into CDRX grain happens [23]. As the formation of sub-grains preferably occurs near the grain boundaries it seems that at least a part of recrystallization is also done by SIBM at low strains. At high strains, however, the gradual evolution of sub-grains is the prevailing mechanism for the appearance of small CDRX grains inside the old grains. These characteristics are similar to the CDRX process which occurs in 304 austenitic and duplex stainless steels [8,9].

As the deformation continues and the strain increases to 0.45 (Fig. 3 (c)), which is located after the peak strain, the number of recrystallized grains increases again. It is evident that the dissociation of original grains by the CDRX grains has progressed and the fraction recrystallized is about 40 %. Further increase in the amount of strain to 0.6, Fig. 3 (d), increases the recrystallized fraction to about 85 %. Some islands of original deformed grains indicate that the microstructure of a material has not been fully recrystallized at 0.6. This is in agreement with the absence of steady-state flow behavior on the flow curve in Fig. 1 (a). It suggests that further deformation is needed to complete the recrystallization process and reach the steady-state deformation. The micrographs

[DOI: 10.22068/ijmse.17.3.60]

show that the same microstructural evolution, i.e. consecutive deformation, DRV, CDRX, has occurred in the δ islands. In most cases, the dynamic recovery has been reported as the only dynamic restoration mechanism for the ferrite phase due to its high SFE. The emergence of new boundaries in the ferrite phase in deformed specimens under different conditions of thermo-mechanical operations, compared with the initial structure (Fig. 1), suggests that CDRX has also occurred in the ferrite phase. The occurrence of dynamic crystallization in the ferrite phase has also been reported by other researchers [24, 25].

The microstructures of deformed samples at 950 °C and strain rate of 0.1 s-1 are shown in Fig. 4. Unlike to Fig. 3 (a), grain boundary serrations and small recrystallized grains are absent in Fig. 4 (a) (ε = 0.15). It appears that the increase in strain rate has decreased the progress of DRV which is responsible for the formation of serrations on the grain boundaries. Probably, the reduction of deformation time due to the increase in the strain rate has led to a limitation of diffusion and the difficulty of dislocations motion. The weakness of DRV at a higher strain rate possibly retards the evolution of sub-grains and therefore postpones CDRX.

Fig. 4 (b) exhibits the delayed initiation of CDRX at a strain of 0.3, which is around the peak of the flow curve in Fig. 1 (b). Similar to the previous observations in Fig. 3, grain dissociation by the well-developed sub-grains seems to be the prevailing mechanism of CDRX. Figs. 4 (c) and 4 (d) indicate that as the amount of deformation rises, the number of new grains increases. By reaching the strain of 0.6, the deformed grains have replaced with the CDRX grains. A comparison between Figs. 3 (d) and 4 (d) suggests further recrystallized fraction but a bit larger grain size at a strain rate of 0.1 s^{-1}. It can be proposed that more deformation heating is responsible for temperature rise and more recrystallization at 0.1 s^{-1}. At low strain rates, however, the heat of deformation is dissipated to the ambient and cannot heat the sample. The higher local temperature in the sample deformed at 0.1 s^{-1} is revealed in a higher recrystallized fraction in γ matrix and δ ferrite islands as well as a bit larger grain size in Fig. 4 (d).

The average grain size of the matrix phase after various conditions of a hot compression test is reported in Table 2. The grain size measurement was carried out alongside and perpendicular to the compression axis and then the average was recorded.

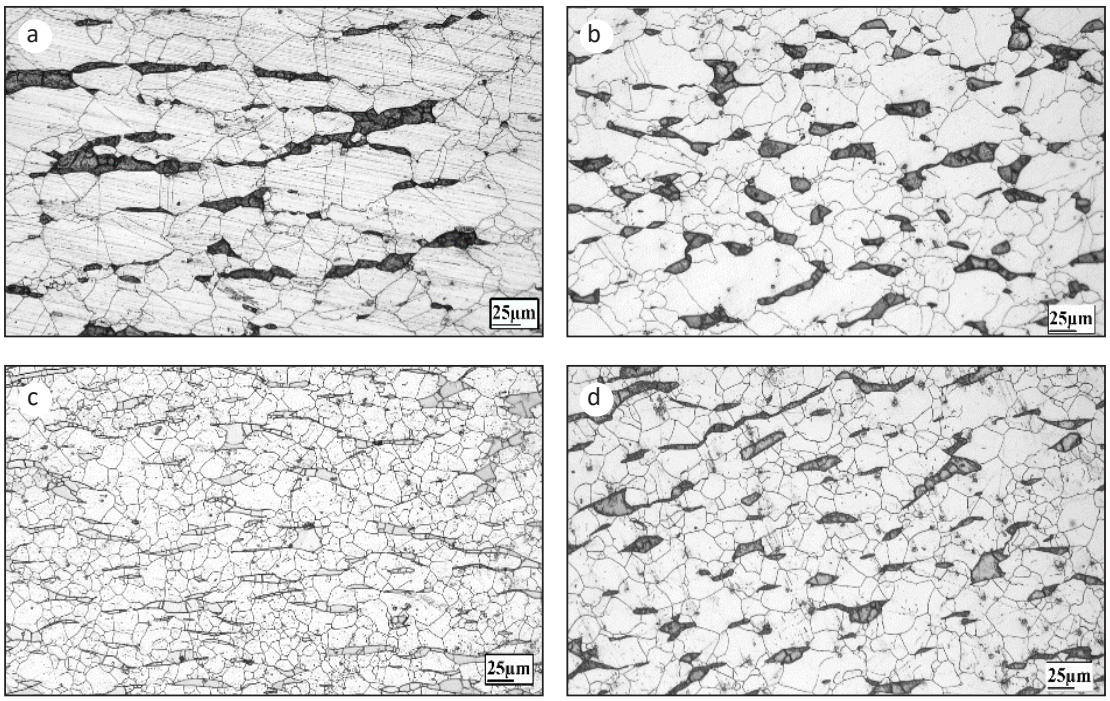

Fig. 4. Microstructure of deformed samples at 950 °C and strain rate of 0.1 s^{-1} to strain a) 0.15, b) 0.3, c) 0.45 and d) 0.6.

[DOI: 10.22068/ijmse.17.3.60]

Table 2. Average austenite grain size after different deformation conditions.

Average grain size (μm)	Average grain size in different directions		Test conditions Temperature (°C) – Strain rate (S^{-1}) - Strain
	Perpendicular to the pressure test (μm)	Parallel to the pressure test (μm)	
41.15	47.02	35.29	950-0.01-0.15
36.51	44.53	28.49	950-0.01-0.3
19.86	23.66	16.06	950-0.01-0.45
13.57	15.51	11.64	950-0.01-0.6
35.71	37.99	33.42	950-0. 1-0.15
29.66	32.81	26.51	950-0. 1-0.3
20.27	21.13	19.42	950-0. 1-0.45
14.83	14.76	14.89	950-0. 1-0.6
40.92	45.07	36.78	1050-0.0 1-0.15
41.53	44.97	38.08	1050-0.0 1-0.3
33.21	34.82	31.59	1050-0.0 1-0.45
29.01	30.69	27.34	1050-0.0 1-0.6

The variations in the average austenite grain size with strain at the strain rates of 0.01 and 0.1 s^{-1} and deformation temperature of 950 °C are shown in Fig. 5. It is observed that with an increase in the amount of strain, the average austenite grain size decreases. This is simply attributed to the progress in the recrystallization of the sample, which was also observed in Figs. 3 and 4. It is worthy to note that even though at low strains of 0.15 and 0.3 deformations at 0.1 s^{-1} leads to finer grain size, at higher strains of 0.45 and 0.5 the accumulation of deformation heating leads to larger grain size at 0.1 s^{-1} with respect to 0.01 s^{-1}. These results also comply with the recrystallization fractions in Figs. 3 and 4.

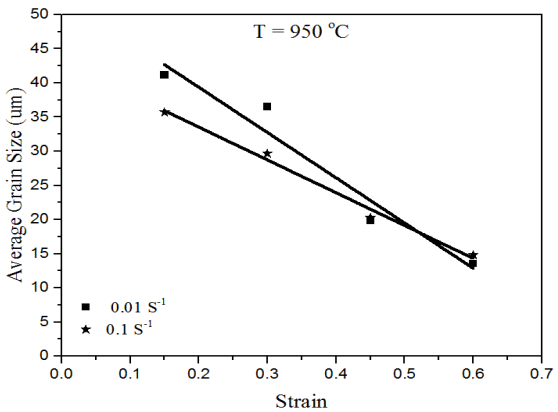

Fig. 5. Variation in the average austenite grain size with strain rate at constant temperature of 950 °C.

The volume fractions of ferrite and austenite after various deformation conditions were determined using the MIP image analyzer software and the results are drawn in Fig. 6. It is evident that with an increase in the amount of strain at both strain rates of 0.01 and 0.1 s^{-1} the volume fraction of the ferrite phase reduces and that of the austenite phase rises. In addition, the role of strain rate on the volume fraction of phases increases with increasing strain. It is inferred that the hot deformation, especially at higher strain rates and larger strains, leads to the strain-induced transformation of ferrite into austenite [26].

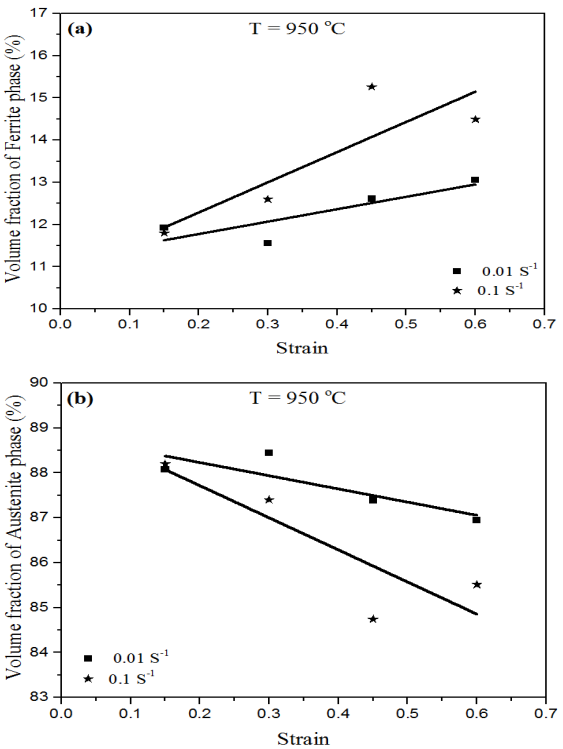

Fig. 6. Changes in the volume fraction of a) ferrite and b) austenite with strain at various strain rates and constant temperature of 950 °C.

[DOI: 10.22068/ijmse.17.3.60]

The microstructures of the deformed samples at 1050 °C and the strain rate of 0.01 s^{-1} are shown in Fig. 7. As seen the austenite grains are considerably refined with an increase in the applied strain. Similar to the micrographs of Fig. 3, the elongation of original grains and formation of new CDRX grains at original grain boundaries or inside the grains are the major microstructural mechanisms which proceed with the applied strain. A comparison between the micrographs of Figs. 3 and 7 show that the fraction recrystallized in 1050 °C is much more than in 950 °C. In addition, larger grain sizes in Fig. 7 suggest that CDRX is followed by grain growth at 1050 °C. The faster kinetics of CDRX at 1050 °C is due to the acceleration of DRV with an increase in the deformation temperature. Besides, it is confirmed that the volume fraction of ferrite increases by an increase in the deformation temperature from 950 to 1050 °C. It should be noticed that, the existence of large δ ferrite islands is a challenge to the hot working of stainless steel. It has been shown that cracking alongside the δ/ γ interphase boundary is a possible failure mechanism through hot working [27]. This challenge is intensified when γ and δ tend to soften by various mechanisms such as DDRX and CDRX. But, the similarity of the DRX mechanism in the γ matrix and δ ferrite islands in the studied material decreases the risk of inhomogeneous deformation. The absence of cracking along the interphase boundary at both temperatures of 950 and 1050 °C confirms this idea.

The variation of average austenite grain size with strain at 950 and 1050 at a constant strain rate of 0.01 s^{-1} is shown in Fig. 8. It is revealed that with increasing strain at both deformation temperatures, the average size of γ matrix decreases. It is also evident that deformation at 1050 °C leads to a larger grain size at all strain values. As aforementioned, the completely recrystallized micrographs in Fig. 7 suggest that grain growth after recrystallization should be the reason for the larger grain size at 1050 °C. The increase in temperature facilitates the diffusion process and thus increases the grain boundary mobility.

Changes in the volume fraction of ferrite and austenite with strain and temperature at a constant strain rate of 0.01 s^{-1} are reported in Fig. 9. In this Fig, it is also observed that the volume fraction of δ ferrite increases with an increase in the deformation temperature from 950 to 1050 °C. This is the rationale because δ ferrite is the

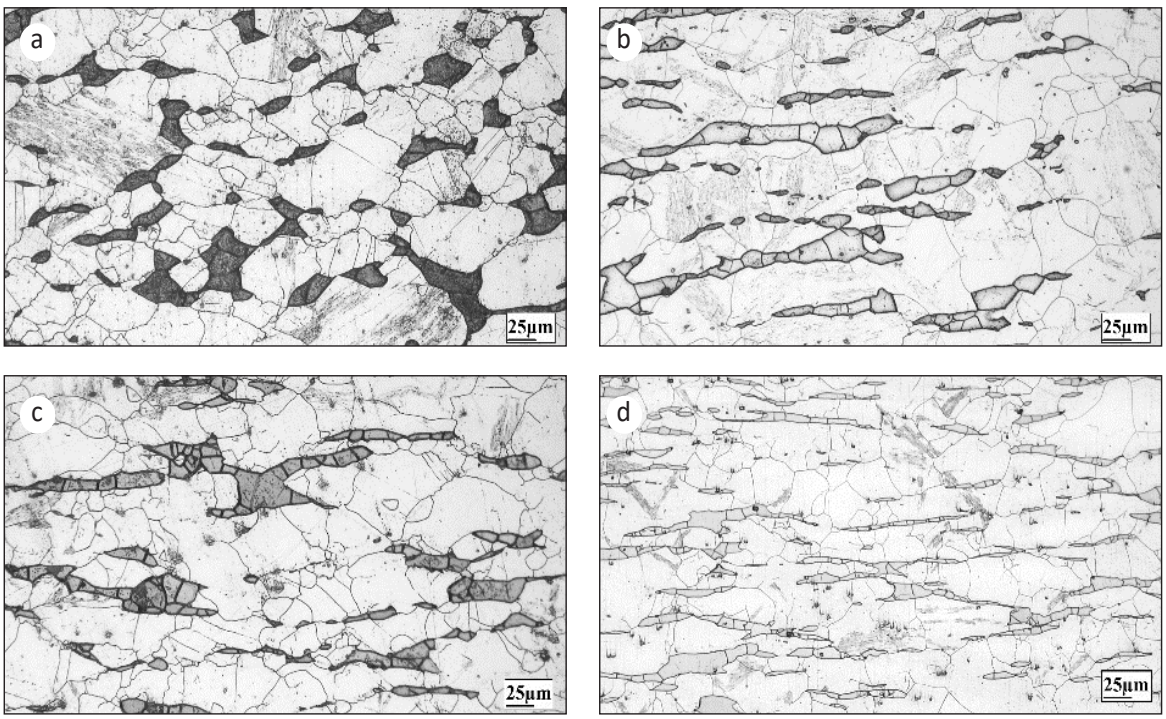

Fig. 7. Microstructure of deformed samples at 1050 °C and strain rate of 0.01 s^{-1} up to strain of a) 0.15, b) 0.3, c) 0.45 and d) 0.6.

[DOI: 10.22068/ijmse.17.3.60]

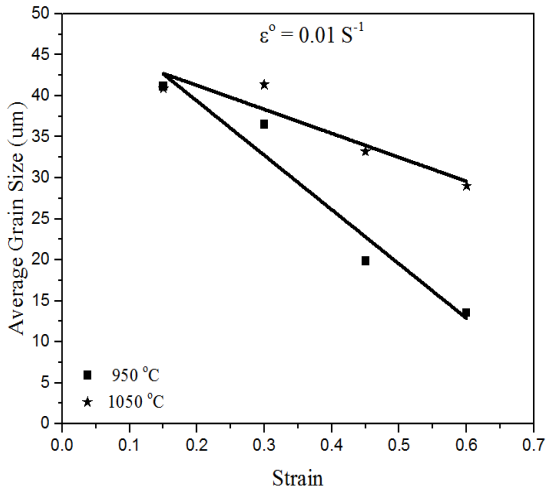

Fig. 8. Variation of the average size of austenite grains with strain and temperature at the constant strain rate of 0.01 s^{-1}.

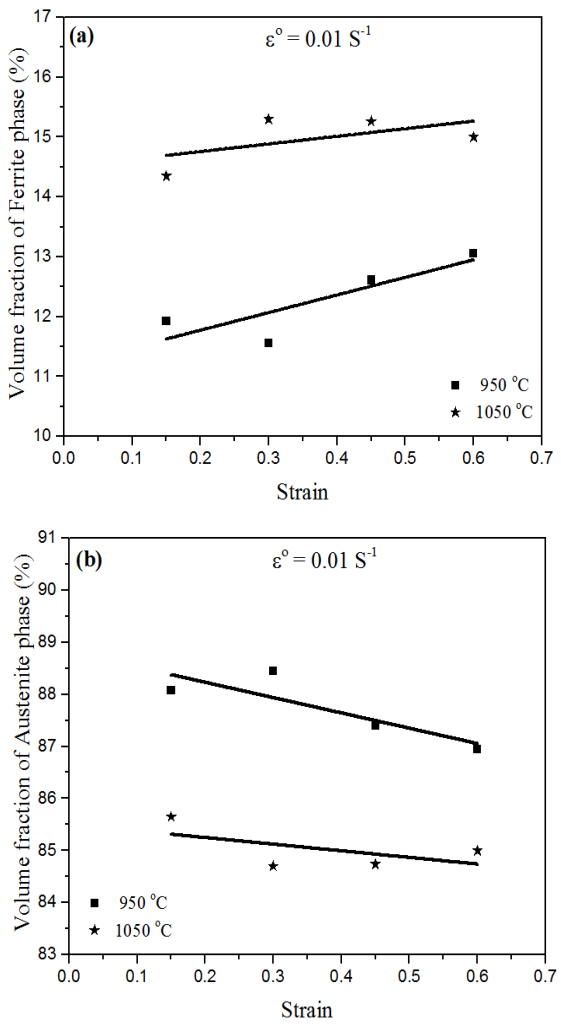

Fig. 9. Changes in the volume fraction of a) ferrite and b) austenite with strain and temperature at constant strain rate of 0.01 s^{-1}.

stable phase at higher temperatures. It is also obvious that the amount of ferrite decreases by an increase in the applied strain due to its transformation into austenite. A comparison between the slopes of curves in Fig. 9 indicates that the rate of δ ferrite to austenite transformation is higher at 950 °C, where ferrite is less stable.

4. CONCLUSIONS

In the present study, the hot-deformation behavior of semi-austenitic precipitation hardening 17-7PH stainless steel was investigated using hot compression tests at 950 and 1050 °C and strain rates of 0.01 and 0.1 s^{-1}. The main results of this research can be summarized as follows:

1. The flow stress of the 17-7PH stainless steel is affected by the thermomechanical parameters (temperature and strain rate). It was found that the flow stress increases with a decrease in the deformation temperature and an increase in the strain rate.
2. In the austenite phase, the reduction in grain size during deformation proves the occurrence of dynamic recrystallization. From the absence of strain-induced grain boundary migration, it was inferred that continuous dynamic recrystallization by the mechanism of rotation of the sub-grains is responsible for the grain refinement.
3. The emergence of new boundaries in the ferrite phase confirms the occurrence of DRX The high stacking fault energy in the ferrite provides the possibility for continuous dynamic recrystallization.
4. It was found that the volume fraction of ferrite decreases with strain during hot working. The rate of this reduction is higher at 950 °C. The strain-induced transformation into austenite can be proposed for the decrease in the amount of ferrite.

REFERENCES

1. McQueen, H. J., and Jonas, J. J., "Recent advances in hot working: Fundamental dynamic softening mechanisms", J. Appl. Metalwork., 1984, 3.3, 233-241.
2. McQueen, H. J., "The production and utility

[DOI: 10.22068/ijmse.17.3.60]

of recovered dislocation substructures", Metal. Trans. A., 1977, 8.6, 807-824.
3. Song, R., D. Ponge, D. Raabe, and Kaspar. R., "Microstructure and crystallographic texture of an ultrafine grained C–Mn steel and their evolution during warm deformation and annealing", Acta Mater., 2005, 53, 845-858.
4. Storojeva, L., Ponge, D., Kaspar, R., and Raabe. D., "Development of microstructure and texture of medium carbon steel during heavy warm deformation", Acta Mater., 2004, 52, 2209-2220.
5. Gourdet, S., and Montheillet. F., "A model of continuous dynamic recrystallization", Acta Mater., 2003, 51, 2685-2699.
6. Eghbali, B., "Effect of strain rate on the microstructural development through continuous dynamic recrystallization in a microalloyed steel", Mater. Sci. Eng. A527, 2010, 15 , 3402-3406.
7. Dehghan-Manshadi, A., and Hodgson. P. D., "Effect of δ-ferrite co-existence on hot deformation and recrystallization of austenite", J. mater. sci., 2008, 43.18, 6272.
8. Yanushkevich, Z., Belyakov, A. and Kaibyshev, R., "Microstructural evolution of a 304-type austenitic stainless steel during rolling at temperatures of 773–1273 K", Acta. Mater., 2015, 82, 244-254.
9. Tsuzaki. K., Xiaoxu. H, and Maki. T., "Mechanism of dynamic continuous recrystallization during superplastic deformation in a microduplex stainless steel", Acta mater, 1996, 44.11, 4491-4499.
10. Cizek, P., "The microstructure evolution and softening processes during high-temperature deformation of a 21Cr–10Ni–3Mo duplex stainless steel", Acta Mater., 2016, 106 , 129-143.
11. Humphreys, F. J. and Hatherly, M., "Recrystallization and related annealing phenomena", Elsevier, 2012.
12. Iza-Mendia, A., Pinol-Juez, A., Urcola, J. J. and Gutierrez, I., "Microstructural and mechanical behavior of a duplex stainless steel under hot working conditions", Metal. Mater Trans. A, 1998. 29, 2975-2986.
13. Marandi, A., Zarei-Hanzaki, R., Zarei-Hanzaki, A. and Abedi, H. R., "Dynamic recrystallization behavior of new transformation–twinning induced plasticity steel", Mater. Sci. Eng. A., 2014. 607, 397-408.
14. Gupta, A., Bhargava, A. K., Tewari, R. and Tiwari, A. N., "TEM studies of boron-modified 17Cr-7Ni precipitation-hardenable stainless steel via rapid solidification route". Metal. Mater. Trans. A., 2013. 44, 4248-4256.
15. Xu, X. L., and Yu. Z. W., "Metallurgical analysis on a bending failed pump-shaft made of 17-7PH precipitation-hardening stainless steel", J. Mater. Process. Tech. 2008, 198, 254-259.
16. Abedi, H. R., A. Zarei Hanzaki, N. Haghdadi, and Hodgson. P. D., "Substructure induced twinning in low density steel", Scr. Mater., 2017, 128, 69-73.
17. Yue, C. X., Zhang, L. W., Liao, S. L., Pei, J. B., Gao, H. J., Jia, Y. W. and Lian, X. J., "Research on the dynamic recrystallization behavior of GCr15 steel", Mater. Sci. Eng. A., 2009, 499, 177-181.
18. Ning, Y., Fu, M. W. and Chen, X., "Hot deformation behavior of GH4169 superalloy associated with stick δ phase dissolution during isothermal compression process", Mater. Sci. Eng. A., 2012, 540, 164-173.
19. Dehghan-Manshadi, A., Beladi, H., Barnett, M. R. and Hodgson, P. D., "Recrystallization in 304 austenitic stainless steel", Mater. Sci. Forum, 2004, 467, 1163-1168.
20. Huang, K., and Logé. R. E., "A review of dynamic recrystallization phenomena in metallic materials", Mater. Design., 2016, 111, 548-574.
21. Bricknell, R. H. and Edington, J. W., "Textures in a superplastic Al-6Cu-0.3 Zr alloy", Acta. Metal., 1979, 27, 1303-1311.
22. Nes, E., "Hot deformation behaviour of particle-stabilized structures in Zr-bearing Al alloys", Metal Science 13.3-4 (1979): 211-215.
23. Abbasi, S. M., Momeni, A., Lin, Y. C. and Jafarian, H. R., "Dynamic softening mechanism in Ti-13V-11Cr-3Al beta Ti alloy during hot compressive deformation", Mater. Sci. Eng. A., 2016, 665, 154-160.
24. Najafi-Zadeh, A., J. J. Jonas, and Yue. S., "Grain refinement by dynamic recrystallization during the simulated warm-rolling of interstitial free steels", Metal. Trans. A., 1992, 23.9, 2607-2617.
25. Longfei. Li, Yang. W., and Sun. Z., "Dynamic recrystallization of ferrite in a low-carbon steel", Metal. Mater. Trans. A., 2006, 37.3, 609-619.

[DOI: 10.22068/ijmse.17.3.60]

26. Sun, L., Muszka, K., Wynne, B. P. and Palmiere, E. J., "Effect of strain path on dynamic strain-induced transformation in a microalloyed steel". Acta Mater., 2014, 66, 132-149.
27. McQueen, H. J., and Jonas. J. J., "Recent advances in hot working: Fundamental dynamic softening mechanisms", J. App. Metalwork., 1984, 3.3, 233-241.

[DOI: 10.22068/ijmse.17.3.60]